

# Measurement of Thickness of Foam layer and Entrance Region in a Bubble Column using Image Processing Technique

Neha Agarwal, Ashok Kumar Verma

**Abstract:** *Photographic method is a direct method for study of bubble behavior. Hydrodynamic study in a rectangular bubble column (0.37m X 0.2m X 0.02m) for air-water system was studied using photographic technique by recording movie at 120fps. Image processing tools were applied to measure regions of gas-liquid dispersion, entrance, foam layer and bubble-bursting were identified. The foam layer thickness showed maxima at  $U_g = 0.1 \text{ m s}^{-1}$ . It decreased with increasing static bed height. The width of entry region also passed through maxima, though it was not sharp. The width of entry region increased with increasing settled bed height. Gas holdup measured in terms of pixel density deviated from experimental values with increasing superficial gas velocity due to overlapping bubbles. The average gas holdup decreased with increasing static bed height.*

**Keywords :** *Bubble column, Gas holdup, Hydrodynamics, Image processing, Multi-phase system.*

## I. INTRODUCTION

Bubble columns (BC) are used in several chemical and biochemical industries for efficient mixing of gas-liquid phases due to its easy and economic construction and operation. Presence of a foam layer as a top layer is quite common in a BC. The foam can be produced by adding a foaming agent or sometimes it is present due to trace impurities either present in the solution or are produced due to chemical and biochemical reactions. Bubbles column has also been used for foam fractionation to remove metals from wastewater [1].

While a vast literature on hydrodynamic parameters such as gas holdup and bubble behaviour influencing performance of BC are available in literature [2-4], literature on foam behaviour in BC are not many [5-8]. Bennet et al. [5] used Electrical Capacitance Tomography (ECT) to clearly identify aerated water, foam and air from local water fractions. Though, foam layer thickness was not measured, the ECT technique was found to be suitable. Veera et al. [6] studied effect of gas velocity on gas holdup in foaming systems.

Yamashita [7] carried out quantitative study in a bubble column of rectangular cross section (0.05 m x 0.10 m). The hole diameter varied from 0.0005 m to 0.008 m. The foam layer thickness,  $f_w$ , was measured by pressure measurement at various axial locations. Following correlation for  $f_w$  for

**Revised Manuscript Received on August 05, 2019.**

**Neha Agarwal**, Department of Chemical Engineering and Technology, Indian Institute of Technology (Banaras Hindu University) Varanasi, India. E-mail: neha.agarwal.che10@itbhu.ac.in.

**Ashok Kumar Verma**, Department of Chemical Engineering and Technology, Indian Institute of Technology (Banaras Hindu University) Varanasi, India. E-mail: akverma.che@itbhu.ac.in.

superficial gas velocity in the range of 0.006 - 0.44  $\text{ms}^{-1}$  was proposed. The constants have been changed to SI units.

$$f_w = 0.433U_g^{0.73} \quad (1)$$

Equation (1) predicts the foam layer thickness to increase monotonically with  $U_g$ . Entrance region thickness,  $e_w$ , was also measured and correlated by the following equations.

$$e_w = 4.8 - 4.8 \log U_g \quad \text{for } F \leq 0.1 \quad (2a)$$

$$e_w = -0.2 - 4.8 \log U_g \quad \text{for } F \geq 0.1 \quad (2b)$$

Equations (2a) and (2b) are converted to SI units. The parameter  $F$  was defined as ratio of innermost width of aerated area containing all the holes to cross-sectional area. A value of 0.1 is close to single nozzle situation. For perforated plate sparger Equation (2b) is applicable.

Pilon et al. [8] have reviewed experimental work on foam layer and reported that the foam layer thickness depends on physical properties of the system, geometrical parameters, bubble radius, temperature and pressure. Steady-state foam thickness,  $f_w$ , in case of highly viscous liquids was correlated by the following equation.

$$f_w = 2905(d_b / 2)Ca^{-1}(Fr/Re)^{1.8} \quad (3)$$

The dimensionless numbers,  $Re$ ,  $Fr$ , and  $Ca$  were defined as

$$Re = \rho_l(d_b / 2)(U_g - U_{gf}) / \mu_l \quad (4a)$$

$$Fr = (U_g - U_{gf})^2 / (gd_b / 2) \quad (4b)$$

$$Ca = \mu_l(U_g - U_{gf}) / \sigma_l \quad (4c)$$

Here,  $U_{gf}$  is the gas velocity at onset of foaming, conditions for which in case of pneumatic foams were reported in a later study [9]. The value of  $U_{gf}$  can easily be obtained by extrapolating the data for  $f_w$  vs  $U_g$  and can be used in Equations (4a) to (4c).

Photographic study of size and shape of the bubbles, bubble velocity is considered as the direct though time consuming method to measure these parameters. Several investigators have started using efficient image processing methods for measuring these parameters [10-19]. The image processing algorithms reported in literature are bubble segmentation and reconstruction techniques [17], watershed algorithm [12,13], algorithm combining geometrical, optical and topological information [14] and recursive algorithm [4] etc. These were applied to process the high-speed bubbly flow images. Bubble size

distribution, bubble shape, transition from homogeneous to turbulent flow, bubble vertical velocity and qualitative behaviour etc. are some of the hydrodynamic parameters reported in literature.

In the present work, an image processing algorithm to measure thickness of entrance region and foam layer using image processing technique to analyse video was developed. The algorithm was used to predict the gas holdup also. The effect of superficial gas velocity and static bed heights on foam layer thickness, entrance layer thickness and gas holdup was studied and are presented.

## II. EXPERIMENTAL SETUP

### A. Experimental Setup

Experimental setup consisted of a rectangular column with 0.37m height, 0.2m width and 0.02m depth. It is shown in Fig. 1 and was made of Perspex sheet. Two walls facing the camera for photographic study were made of glass to avoid erosion of the wall and facilitate easy cleaning.

Air was sparged through a distributor to provide uniform bubbling. The sparger consisted of a perforated plate having 200 holes of 0.0015 m diameter. Over it 0.005 m glass beads were filled upto a height of 0.05 m. A 200 mesh of SS was placed over the beads. The glass beads between the perforated plate and mesh acted as calming section. The bubble column consisted of a conical bottom below the perforated plate. The gas was supplied using a compressor. The flow rate of the gas was measured by a rotameter.

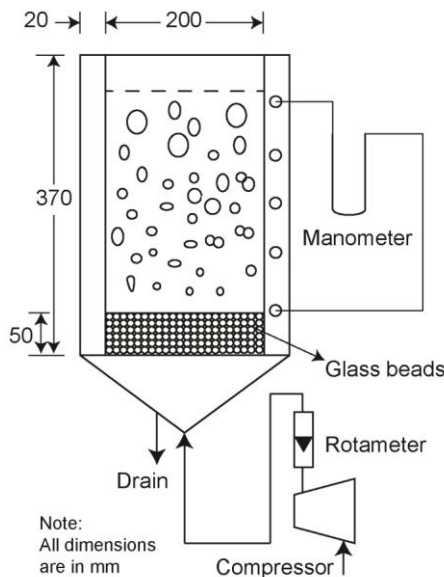


Fig. 1. Experimental set-up

Light sources (100 watt bulbs) were placed behind the rear wall which was covered with a translucent plastic sheet to diffuse the light resulting in almost uniform illumination. A Nikon (J4 model) camera was mounted on a stand in front of the wall at a height equal to center of the column and at a distance of 1.5 m from it. After some prearrangements of

camera position, backlight illumination of the column and use of a regulated power supply resulted in similar illumination in all the frames. To achieve this, the set-up was surrounded by walls to avoid reflections from the column walls. The camera was synchronized to record at a rate of 120 fps.

### B. Experimental Procedure

Air was bubbled through water and the flow rate of air was measured using a rotameter. Camera was switched on to record video at 120 fps for 3 seconds. Such recordings were made at several superficial gas velocity and static bed height. The bubbles looked as dark rings and bright centers. Some overlapping of bubbles was also observed at high gas velocity.

Later the videos were processed using an image processing algorithm written in MATLAB. The image was enhanced by a series of image processing techniques as given below. The enhanced image was analysed to identify entrance region, foam layer and expanded bed height,  $H_e$  and measure each of them. An average over 60 successive frames were taken and are presented. The gas holdup was estimated from the values of  $H_e$ . The image processing algorithm used in this work consisted of the following steps.

1. A frame from video was extracted and cropped to contain active test section only (Fig. 2a).
2. Range filtering was applied to characterize regions of image by their texture content. Statistical measure as range provides information about the local variability of the intensity values of pixels in an image.
3. Filtered image was converted to grayscale image.
4. Background noise was minimized. Salt-pepper noise was removed with the help of nonlinear digital filtering technique known as median filtration.
5. Enhancement of the image was carried out by adjusting the image contrast.
6. Histogram equalization of the image was performed to enhance the contrast of images by transforming the values in an intensity image.
7. Threshold was applied to the image.
8. Obtained image was converted into binary image (Fig. 2b).

The binary image was used to extract feature of the gas-liquid dispersion in the bubble column. In this image the white pixels correspond to bubbles. Black pixels outside bubbles correspond to liquid. Black pixels inside the bubble do not necessarily represent presence of liquid. From the binary images pixel density has been defined as fraction of white pixels to all the pixels at any particular height above the distributor plate. The procedure is completely independent of bubble shape and its size, but only depends on the image processing technique implemented to perform phase discrimination.

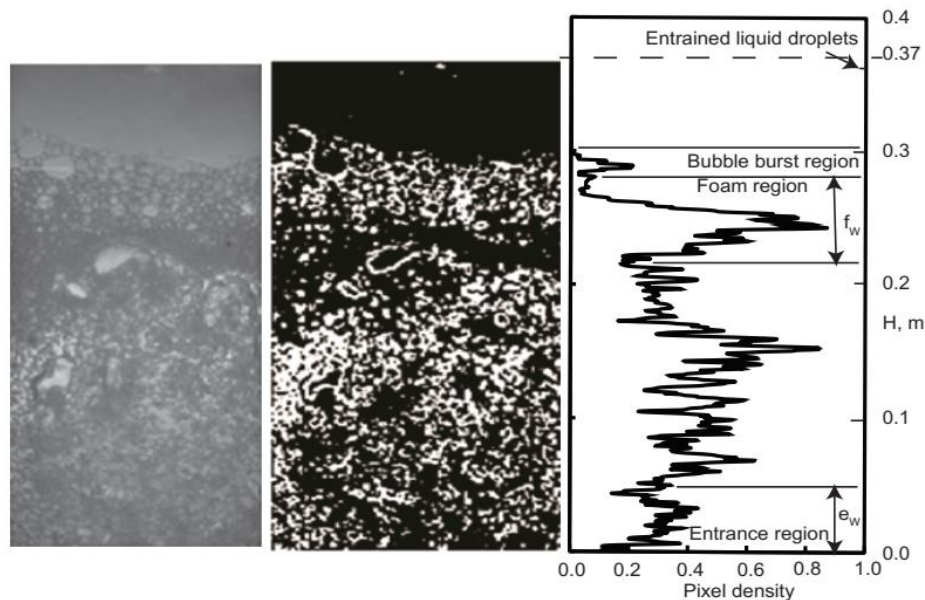


Fig. 2. Image of air-water dispersion in bubble column (a) on left-original image (b) in middle-final binary image (c) on right-Pixel density at different position above distributor plate

### III. RESULTS AND DISCUSSION

Visual observation of the bubble column had indicated the presence of a foam layer at the top with few bubble burst resulting in entrainment of the liquid above the air-water dispersion. Due to rapid variation of bed height it was not possible to measure the foam layer manually. It was even more difficult in the case of entry region.

#### A. Pixel Density in Vertical Direction

Variation of pixel density as a function of height above the distributor plate for superficial gas velocity,  $U_g = 0.105 \text{ m s}^{-1}$  and static bed height,  $H_s = 0.145 \text{ m}$  (corresponding to the image in Fig. 2a) is shown in Fig. 2c. Bottom of the binary image corresponds to the region adjacent to the sparger. The top of the image is black due to absence of liquid. Presence of small isolated value of pixel density at a height,  $H = 0.37 \text{ m}$  is attributed to entrainment of liquid after bursting of air bubble. The top surface of the bed was not horizontal. The height at which last peak obtained was taken as the value of average expanded bed height in each frame.

Variation of pixel density with  $H$  is not smooth. It shows an increasing trend above the sparger and in most of the video-frames there is a distinct drop in pixel density at about

$H=0.4 \text{ m}$ . On comparison with the image (Fig. 2a) it was decided to take this height as the thickness of the entry region. The pixel density shows an increasing trend with increasing value of  $H$ . Near the top at about  $H=0.22 \text{ m}$  a sudden drop in pixel density was observed. It again increases, passes through a maximum value and decreases. It was observed in all the cases and was attributed to the presence of a foam layer after comparing with the image. In some cases a small peak again appears. It was due to bursting of bubble and was included while estimating the expanded bed height.

Variation of pixel density along the height of the column at  $H_s=0.15 \text{ m}$  for three values of  $U_g = 0.042, 0.084$  and  $0.168 \text{ m s}^{-1}$  are presented in Fig. 3 (a) through (c). The trend for all values of  $U_g$  is similar to that presented in Fig. 2. The increase in pixel density in lower portion of the column is gradual. The decrease in pixel density at  $H > 0.15 \text{ m}$  becomes less sharp with increasing  $U_g$ . Beyond the expanded bed height,  $H_e$ , i.e. at  $H > H_e$ , the pixel density drops to a very small value showing absence of any bubbles.

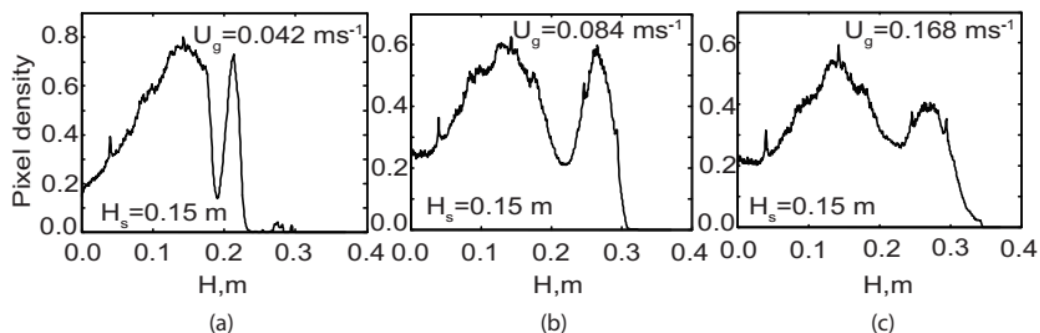


Fig. 3. Effect of  $U_g$  on pixel density as a function of  $H$  at (a)  $U_g = 0.042 \text{ m s}^{-1}$  (b)  $U_g = 0.084 \text{ m s}^{-1}$  (c)  $U_g = 0.168 \text{ m s}^{-1}$

**B. Foam Layer Thickness**

The foam layer width,  $f_w$ , was estimated from graphs of pixel density as a function of  $H$  for 60 successive frames (corresponds to 0.5 s). Average values of  $f_w$  are presented in Table 1.

Table 1.  $f_w$  as a function of  $U_g$  and  $H_s$

$U_g, \text{ms}^{-1}$	$f_w \times 10^2, \text{m}$								
	13.	13.	14.	14.	15.	15.	16.	16.	17.
0.04			3.		4.		3.		
2	5.3	3.7	8	3.4	3	3.7	8	3.4	5.3
0.06			6.		6.		5.		
3	9.1	6.9	1	6.1	4	5.5	2	5.4	9.1
0.08	10.		8.		6.		5.		10.
4	8	8.2	2	7.4	7	6.1	7	5.6	8
0.10	10.		9.		6.		5.		10.
5	8	9.9	0	8.4	9	6.4	9	5.7	8
0.12	9.8		9.		6.		6.		
6	3	9.6	1	8.0	7	6.0	0	6.1	9.8
0.14	8.6		7.		6.		5.		
7	8	8.4	7	7.6	2	4.4	5	5.0	8.7
0.16	7.0		6.		5.		4.		
8	5	6.4	9	6.4	1	2.5	8	3.6	7.1

Present values of  $f_w$  at  $H_s = 0.135 \text{ m}$  as a function of  $U_g$  are compared with correlations of Yamashita[7] and Pilon et al. [8] are compared in Fig. 4. While using Equation 3, the gas velocity at which onset of foaming occurs was determined by fitting the present data by a second order polynomial and extrapolating it to the x-axis where  $f_w = 0$ . The extrapolation is shown by the dotted line. The value of bubble diameter was taken as 0.004 m as measured from photographically. The value of  $U_{gf}$  thus estimated is  $0.064 \text{ m s}^{-1}$ . Both correlations show monotonically increasing value of  $f_w$ . At  $U_g = 0.042 \text{ m s}^{-1}$  the present value is in close agreement to the values predicted by both correlations. The methodology developed to measure the foam layer thickness is thus validated. The values of  $f_w$  estimated from Equation 1 and 3 increased to 0.118 m and 0.132 m respectively at  $U_g = 0.168 \text{ ms}^{-1}$ . In the present study it showed a maximum value of 0.061 m at  $U_g = 0.126 \text{ m s}^{-1}$ . The deviation at higher gas velocity may be due to the change in bubble diameter. The foam layer thickness is known to be very sensitive to the bubble radius [8].

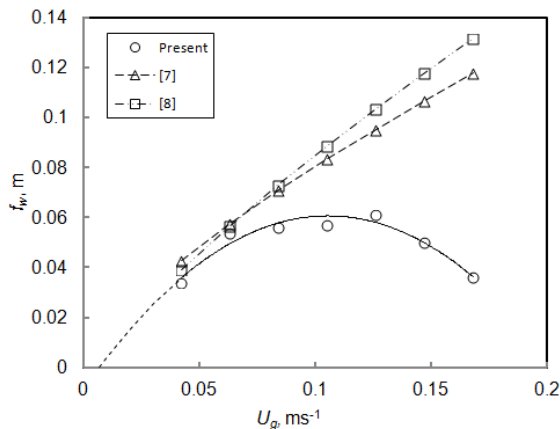


Fig. 4. Comparison of  $f_w$  with correlations of Yamashita [7] and Pilon et al. [8].

The values of  $f_w$  as a function of  $U_g$  and  $H_s$  are presented in Fig 5. The foam width increases with increasing  $U_g$  upto a

value of  $U_g = 0.1 \text{ ms}^{-1}$  above which it starts decreasing. This trend was observed at all values of  $H_s$ . The effect became less prominent as the value of  $H_s$  increased. This trend is not in accordance with the results of Yamashita [7] who found that the foam layer thickness increases monotonically with increasing gas velocity. The maximum foam width decreased with increasing value of  $H_s$ . Yamashita [7] measured foam layer thickness for  $H_s$  in the range of 0.5 m – 0.79 m, which is almost double as compared to the value  $H_s$  used in the present study. It indicates that the foam layer thickness may not follow monotonic increasing trend at low values of  $H_s$ .

The gas velocity at which maximum foam thickness is same as the velocity upto which uniform bubbling occurs i.e. upto  $U_g < 0.1 \text{ m s}^{-1}$ . During transition from uniformly bubbly regime to churn turbulent regime the foam layer thickness decreases. Present experimental conditions did not cover a wide range of churn-turbulent conditions. As only small bubbles are present at low  $U_g$ , the bubbles do not get sufficient time for coalescence to take place and leave the column before it could happen. At large values of  $U_g$  bubble coalescence takes place. It results in formation of large bubbles which move at large velocity and burst at the top. As a result the foam layer decreases. The present data is at low value of  $H_s$  and hence the present trend is applicable to shallow beds only.

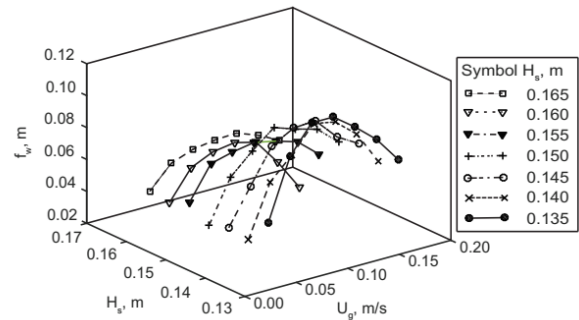


Fig. 5.  $f_w$  as a function of  $U_g$  and  $H_s$

**C. Entry Region Width**

The entry region width,  $e_w$ , was estimated from pixel density as an average over 60 frames. Average value of  $e_w$  are presented in Table 2.

Table 2.  $e_w$  as a function of  $U_g$  and  $H_s$

$U_g, \text{ms}^{-1}$	$e_w \times 10^2, \text{m}$								
	13.	13.	14.	14.	15.	15.	16.	16.	17.
0.04	3.		3.		3.		4.		3.
2	0	3.2	3	3.4	4	3.9	2	4.2	0
0.06	4.		4.		4.		4.		4.
3	4	4.4	4	4.4	4	4.4	4	4.4	4
0.08	4.		4.		4.		4.		4.
4	4	4.5	5	4.5	4	4.5	6	4.7	4
0.10	4.		4.		4.		4.		4.
5	4	4.5	5	4.7	8	4.9	9	5.0	4
0.12	4.		4.		4.		5.		4.
6	5	4.6	6	4.7	8	4.9	2	5.2	5
0.14	4.		4.		4.		4.		4.
7	7	4.8	8	4.8	9	4.8	9	5.0	7
0.16	4.		3.		4.		4.		4.
8	4	4.6	9	4.4	2	4.5	5	4.5	4



Variation of  $e_w$  with  $H_s$  and  $U_g$  is presented in Fig. 6. The width of entry region increases with increasing settled bed height. It increases upto  $U_g = 0.084 \text{ ms}^{-1}$ . Above this value at low values of  $H_s$ , the value of  $e_w$  remains constant. It decreases at large value of  $U_g$ . The trend is same at all values of  $H_s$ . The present trends do not follow monotonic increase of entrance layer as predicted by Equation (2b) [7].

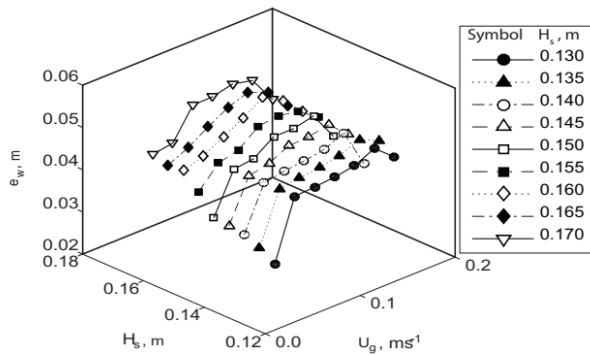


Fig. 6.  $e_w$  as a function of  $U_g$  and  $H_s$

#### D. Gas Holdup

Experimental values of gas holdup were estimated by following equation.

$$\epsilon_g = (H_e - H_s) / H_e \quad (5)$$

Where  $H_e$  is average bed height measured from the images as discussed above. The gas holdup was also measured from pixel density in the expanded bed region by using the following relation.

$$\epsilon_{pixel} = \text{Pixels occupied by bubbles} / \text{Total pixels} \quad (6)$$

A comparison between gas holdup calculated by height measurement and pixel intensity is presented in Fig. 7. At lower values both values are in close agreement. It may be attributed to absence of overlapping bubbles or insignificant number of overlapping bubbles. At high gas velocity, the gas holdup is high and the number of overlapping bubbles is significant. Therefore,  $\epsilon_{pixel}$  was lower than  $\epsilon_g$ . In the region of overlapping bubbles, the error in estimation of gas holdup is less than 10 %.

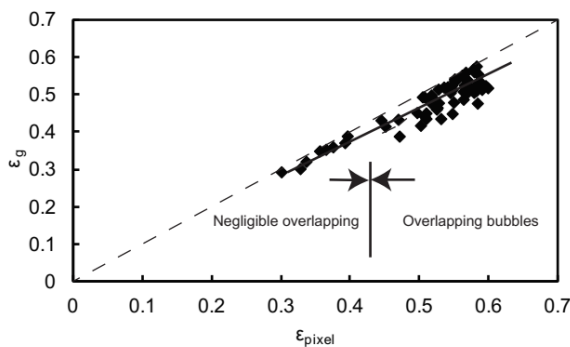


Fig. 7. Comparison of  $\epsilon_g$  and  $\epsilon_{pixel}$

From binary images values of  $\epsilon_{pixel}$  were estimated and corrected with the correlation coefficient to estimate the values  $\epsilon_g$ . The values of  $\epsilon_g$  as a function of  $U_g$  and  $H_s$  are presented in Fig. 8 and Table 3.

Table 3. Gas holdup as a function of  $U_g$  and  $H_s$

$U_g, \text{ms}^{-1}$	$H_s \times 10^2, \text{m}$									
	13	13.	14	14.	15	15.	16	16.	17	17
0.04	0.5	0.4	0.4	0.4	0.3	0.4	0.3	0.3	0.2	0.2
2	1	9	7	5	4	1	2	0	9	
0.06	0.5	0.5	0.5	0.4	0.4	0.4	0.4	0.4	0.3	
3	4	2	0	9	4	6	3	1	9	
0.08	0.5	0.5	0.5	0.5	0.5	0.5	0.4	0.4	0.4	
4	7	5	3	2	0	1	9	6	3	
0.10	0.5	0.5	0.5	0.5	0.5	0.5	0.5	0.4	0.4	
5	9	7	5	4	4	3	2	8	6	
0.12	0.5	0.5	0.5	0.5	0.5	0.5	0.5	0.4	0.4	
6	9	8	6	5	5	4	3	9	7	
0.14	0.6	0.5	0.5	0.5	0.5	0.5	0.5	0.4	0.4	
7	0	9	6	6	5	4	3	9	7	
0.16	0.6	0.5	0.5	0.5	0.5	0.5	0.5	0.4	0.4	
8	0	9	7	6	5	5	3	9	7	

The gas holdup increases with increasing gas velocity. The increase is sharp at low gas velocity. Above the transition velocity ( $U_g \approx 0.1 \text{ ms}^{-1}$ ), bubble coalescence takes place and hence gas holdup increase is less sharp. The gas holdup is much higher than that estimated from various correlations in literature. It may be attributed to the presence of significant foam layer.

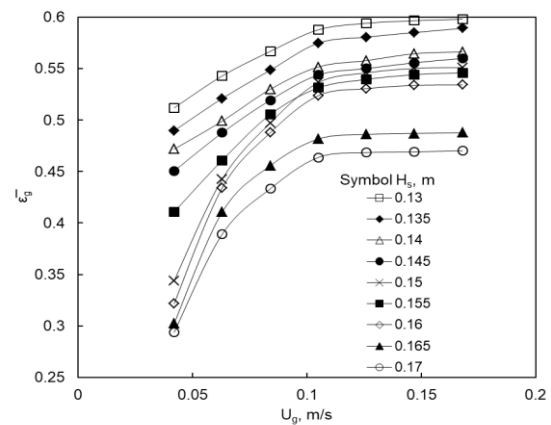


Fig. 8.  $\epsilon_g$  as a function of  $U_g$

#### IV. CONCLUSION

Hydrodynamic aspects of a rectangular bubble column were studied using image processing technique. Using image processing tools, regions of gas-liquid dispersion at the entry and bulk, foam and bubble bursting were observed. Following conclusions were observed.

1. The foam layer thickness,  $f_w$ , showed maxima at  $U_g = 0.1 \text{ m s}^{-1}$ . It was less pronounced at high values of  $H_s$ .
2. Width of entry region also showed a maxima around  $U_g = 0.1 \text{ m s}^{-1}$ . It increased with increasing static bed height.
3. Gas holdup measured in terms of pixel density deviated slightly from experimental values with increasing  $U_g$ . The values of  $\epsilon_{pixel}$  were corrected to obtain the values of  $\epsilon_g$ .
4. Gas holdup increased with increasing  $U_g$  at a given value of  $H_s$ . The values of  $\epsilon_g$  decreased with increasing value of  $H_s$ . It may be due to decrease in relative contribution of foam layer and entry region width.

## ACKNOWLEDGMENT

The authors would like to thank the Department of Chemical Engineering and Technology, Indian Institute of Technology (Banaras Hindu University) Varanasi for the all the supports needed to complete this work.

## REFERENCES

1. Y. Bando, T. Kuze, T. Sugimoto, K. Yasda, M. Nakamura, "Development of Bubble Column for Foam Separation". *Korean J. Chem. Eng.* vol. 17(5), 2002, pp.597-599.
2. Verma, A. K. "Process Modeling and Simulation in Chemical, Biochemical and Environmental Engineering". CRC Press, 2014, Boca Raton.
3. C. Leonard, J. H. Ferrasse, O. Boutin, S. Lefevre, A. Viand, "Bubble column reactors for high pressures and high temperatures operation", *Chem. Eng. Res. Des.* vol. 100, 2015, pp.391-421.
4. S. Zhong, X. Zou, Z. Zhang, H. Tian, "A flexible image analysis method for measuring bubble parameters". *Chem. Eng. Sci.* vol. 141, 2016, pp.143-153.
5. M. A. Bennet, R. M. West, S. P. Luke, R. A. Williams, "The investigation of bubble column and foam processes using electrical capacitance tomography", *Miner. Eng.* vol. 15, 2002, pp.225-235.
6. U. P. Veera, K. L. Kataria, J. B. Joshi, "Effect of superficial gas velocity on gas hold-up profiles in foaming liquids in bubble column reactors", *Chem. Eng. J.* vol. 99, 2004, pp.53-58.
7. F. Yamashita, "Effect of Foam Layer on Gas Holdup in a Bubble Column". *J. Chem. Eng. Jpn.* vol. 28(6), 1995, pp.837-840.
8. L. Pilon, A. G. Fedorov, R. Viskanta, "Steady-State Thickness of Liquid-Gas Foams", *J. Colloid Interface Sci.* vol. 242, 2001, pp.425-436.
9. L. Pilon, R. Viskanta, "Minimum Superficial Gas Velocity for onset of Foaming", *Chem. Eng. Process.* vol. 43, 2004, pp.149-160.
10. A. Karn, C. Ellis, R. Arndt, J. Hong, "An integrative image measurement technique for dense bubbly flows with a wide size distribution", *Chem. Eng. Sci.* vol. 122, 2015, pp.240-249.
11. F. S. Ahmed, B. A. Sensenich, S.A. Gheni, D. Znerdstrovic, M. H. Al-Dahhan, "Bubble Dynamics in 2D Bubble Column: Comparison between highspeed camera imaging analysis and 4-point optical probe", *Chem. Eng. Commun.* vol. 202, 2013, pp.85-95.
12. Y. M. Lau, N. G. Deen, J. A. M. Kuipers, "Development of an image measurement technique for size distribution in dense bubbly flows", *Chem. Eng. Sci.* vol. 94, 2013, pp.20-29.
13. Y. M. Lau, K. T. Sujatha, M. Gaeini, N. G. Deen, J. A. M. Kuipers, "Experimental study of the bubble size distribution in a pseudo-2D bubble column", *Chem. Eng. Sci.* vol. 98, 2013, pp.203-211.
14. Y. Fu, Y. Liu, "Development of a robust image processing technique for bubbly flow measurement in a narrow rectangular channel", *Int. J. Multiphase Flow.* vol. 84, 2016, pp. 217-228.
15. G. Besagni, F. Inzoli, "Comprehensive experimental investigation of counter-current bubble column hydrodynamics: Holdup, flow regime transition, bubble size distributions and local flow properties", *Chem. Eng. Sci.* vol. 146, 2016, pp.259-290.
16. G. Besagni, F. Inzoli, "Bubble size distributions and shapes in annular gap bubble column", *Exp. Therm Fluid Sci.* vol. 74, 2016, pp.27-48.
17. Zaruba, E. Krepper, H. M. Prasser, E. Schleicher, E. "Measurement of bubble velocity profiles and turbulent diffusion coefficients of the gaseous phase in rectangular bubble column using image processing", *Exp. Therm. Fluid Sci.* vol. 29, 2005, pp.851-860.
18. J. R. V.Cordero, D. Samano, R. Zenit, R. "Study of the properties of bubbly flows in Boger-type fluids", *J. Non-Newtonian Fluid Mech.* vol. 175-176, 2012, pp.1-9.
19. S. Amirmia, J. R. deBruyn, M. A. Bergougnou, A. Margaritis, "Continuous rise velocity of air bubbles in non-Newtonian biopolymer solutions", *Chem. Eng. Sci.* vol. 94, 2013, pp. 60-68.
20. G. Besagni, F. Inzoli, G. D. Guido, L. A. Pellegrini, "Experimental investigation on the influence of ethanol on bubble column hydrodynamics", *Chem. Eng. Res. Des.* Vol. vol. 112, 2016, pp.1-15.
21. S. Sasaki, K. Hayashi, K., A. Tomiyama, "Effects of liquid height on gas holdup in air-water bubble column", *Exp. Therm. Fluid Sci.* vol. 72, 2016, pp.67-74.

## AUTHORS PROFILE



**Neha Agarwal** is research scholar in the Department of Chemical Engineering and Technology at Indian Institute of Technology (Banaras Hindu University) Varanasi. She has obtained his M.E degree from IIT (BHU) Varanasi. She is currently working on measurement of bubble behavior in bubble columns using image processing tools for photographic method.



**Ashok Kumar Verma** is professor in the Department of Chemical Engineering and Technology at the Indian Institute of Technology (Banaras Hindu University) Varanasi. He holds a BSc from Allahabad University, a BE in chemical engineering from University of Roorkee (now Indian Institute of Technology, Roorkee), an ME in chemical engineering from the Indian Institute of Sciences, Bangalore, and a PhD in chemical engineering from the Indian Institute of Technology, Kanpur. He joined the Institute of Technology, Banaras Hindu University, Varanasi in 1984. He worked at University of Chicago, Illinois, USA for post-doctoral research during 1987-88. He is author of book "Process Modelling and Simulation in Chemical Biochemical and Environmental Engineering" published by CRC press, Boca Raton, USA. He has also authored or co-authored numerous papers/book chapters in journals, and national and international proceedings. He has presented papers in national and international conferences. His current research area includes application of acoustic signal analysis, image processing and artificial intelligence in various fields of chemical engineering, modelling and simulation of multiphase systems.